Causes and impacts of changes in the Arctic freshwater budget during the 20th and 21st centuries in an AOGCM

Olivier Arzel, T. Fichefet, H. Goosse, Jean-Louis Dufresne

Causes and impacts of changes in the Arctic freshwater budget during the 20th and 21st centuries in an AOGCM

Olivier Arzel[1], Thierry Fichefet[2], Hugues Goosse[2] and Jean-Louis Dufresne[3]

submitted to Climate Dynamics

[1]*Corresponding author address: Climate and Environmental Dynamics Laboratory, School of Mathematics and Statistics, University of New South Wales, NSW 2052, Sydney, Australia, e-mail: o.arzel@unsw.edu.au, fax:* +61 2 93857123

[2]*Institut d'Astronomie et de Géophysique G. Lemaître, Université catholique de Louvain, 2 Chemin du Cyclotron, 1348 Louvain-la-Neuve, Belgium.*

[3]*Laboratoire de Météorologie Dynamique, Institut Pierre Simon Laplace UPMC/CNRS, 4, place Jussieu, Paris, France.*

Abstract

The fourth version of the atmosphere-ocean general circulation model developed at the Institut Pierre-Simon Laplace (IPSL-CM4) is used to investigate the mechanisms influencing the Arctic freshwater balance in response to anthropogenic greenhouse gas forcing. The impacts of these changes on deep mixing in the northern North Atlantic are also studied on the basis of correlation and regression analyses of detrended variables. It is found that the mechanism of inter-annual changes in deep mixing differ fundamentally between the 20th and 21st centuries. This difference is caused by the strong influence of the inter-annual variability of the freshwater export at Fram Strait, and of the freshwater import from the North Atlantic during the 21st century. The model shows that the Fram Strait outflow, which is an important source of freshwater for the northern North Atlantic, experiences a rapid and strong transition from a weak state toward a relatively strong state during 1990-2010. The authors propose that a positive feedback in the atmosphere-sea ice-ocean system in the GIN-Barents Seas sector initiated by the retreat of the sea ice cover in the Barents Sea as a result of the long-term warming of the Arctic climate during the late 20th century is responsible for this behaviour. Around year 2080, the model predicts a second transition threshold beyond which the Fram Strait outflow is restored toward its original weak value. The long-term freshening of the GIN Seas is invoked to explain this rapid transition.

1. Introduction

The freshwater supply to the Arctic Ocean plays a key role in controlling the circulation and water mass properties of this ocean, and the export of this freshwater toward the convection sites located in the Labrador and Greenland-Iceland-Norwegian (GIN) Seas significantly affects deep water formation (e.g., Manabe and Stouffer, 1995, Hakkinen, 1999, Jungclaus et al., 2005) and ultimately the Atlantic meridional overturning circulation (AMOC). Excessive freshwater input to the Arctic Ocean and Nordic Seas could thus influence the climate of the North Atlantic area by decreasing the northward ocean heat transport associated with the large-scale AMOC (e.g., Vellinga and Wood, 2002; Fichefet et al., 2003). It is therefore crucial to analyse the mechanisms of freshwater release from the Arctic Ocean towards sub-Arctic regions on decadal and longer timescales. In particular, this study aims to increase our understanding of the interrelation between changes in freshwater transport toward the convection sites and deep mixing in response to enhanced greenhouse gas conditions.

During the last few decades, the physical Arctic environment has undergone large changes, as reviewed in recent literature (e.g., Serreze et al., 2000; Moritz et al., 2002; Overland et al., 2004). For example, since the mid-60s, the annual mean Arctic surface air temperature has raised by about 2°C. Since the late 70s, satellite records show a decreasing linear trend in Arctic sea ice extent at an annual mean rate of about 0.3 10^6 km^2 per decade (Cavalieri et al., 2003). Submarine-based observations indicate that the sea ice thickness in deep-water areas of the Arctic Ocean has decreased by about 1.3 m in average between 1958-1976 and 1993-1997 (Rothrock et al., 1999). River monitoring data show that the average annual discharge of freshwater from the six largest Eurasian rivers to the Arctic Ocean has increased by about 7% from 1936 to 1999, suggesting an increase of precipitation over land in high latitudes of the Northern Hemisphere during that period (Peterson et al., 2002). Hansen et al. (2001) reported that the cold, dense overflows across the

Greenland-Scotland ridge that feeds the southward branch of the AMOC, has decreased by at least 20 percent during 1950-2000. Dickson et al. (2002) presented evidence of a rapid and sustained freshening of the system of overflows and entrainment that ventilate the deep Atlantic Ocean over 1965-2000. Curry et al (2003) found systematic freshening over much of the water column at both poleward ends of the Atlantic Ocean accompanied by large increases of salinity in the upper water column at low latitudes between the 1950s and the 1990s. Recently, Curry et al. (2005) estimated that the Nordic Seas and the sub-polar basins were diluted by an extra 19,000±5,000 km^3 of freshwater input between 1965 and 1995, with about half of this freshwater being added in the late 60s at a rate of 2,000 km^3 per year during the Great Salinity Anomaly (GSA) event (Dickson et al., 1988).

Whether the high-latitude freshening observed during the past four decades and the reduced overflows are a manifestation of a weakening of the AMOC remains very controversial. Indeed, the relationship between the large-scale AMOC and the northern North Atlantic freshening is difficult to infer from current observations because of the lack of data and the too short period of measurements compared to timescales of internal variability. Nevertheless, Bryden et al. (2005) suggested recently that the AMOC has slowed down by about 30 percent between 1957 and 2004 using five hydrographic trans-Atlantic sections at 25°N. However, these sections have been performed at different seasons during the year, and we can therefore not exclude that the downward trend of the AMOC reported by these authors be due to a large intra-seasonal variability that overwhelms the long-term signal. Using the HadCM3 climate model running over the 20^{th} century, Wu et al. (2004) reported a deep freshening trend of the Labrador Sea similar to that seen in observations by Dickson et al. (2002), and obtained yet an enhancement of the AMOC instead of a weakening. The situation is however very different over the 21^{st} century for which the radiative forcing is much larger than the one experienced over the second half of the past century. In this case models show unequivocally, albeit with various magnitudes, a weakening of the AMOC in response

to increasing anthropogenic greenhouse gas forcing (e.g., Houghton et al., 2001; Fichefet et al., 2003, Gregory et al., 2005). It is worth noting that in all models used in the Coupled Model Intercomparison Project (CMIP), the AMOC weakening is caused more by changes in surface heat flux than by changes in surface freshwater flux (Gregory et al., 2005). However, increase in both sea ice melting and river flows are generally found in these climate-change scenarios, leading to an increase in the freshwater storage of the Arctic/sub-Arctic regions. As a result, the high-latitude ocean stratification increases and the water mass transformation becomes much less efficient, thus contributing to the AMOC weakening.

Although models agree that the northern North Atlantic freshens in response to global warming, the mechanisms driving the changes in freshwater release from the Arctic Ocean to the Nordic Seas and the sub-polar basin of the North Atlantic are still not well understood. Furthermore, the interrelation between changes in deep convection and the freshwater supply to the northern North Atlantic in a warming climate is still not established. This paper arises then from the desire to gain insights into the mechanisms underlying the freshening of the high-latitudes of the Northern Hemisphere, and its link with changes in deep mixing in response to enhanced greenhouse gas conditions. The analysis is based on outputs of simulations performed with an atmosphere-ocean general circulation model (AOGCM) for the fourth assessment report of the Intergovernmental Panel on Climate Change (IPCC AR4). In this paper, we discussed results from the experiment covering the 20th century with anthropogenic forcings and the A1B scenario for the 21st century, which corresponds to an increase of $C0_2$ until a level of 720 ppm by 2100 as defined by the Special Report on Emission Scenario (SRES). It should be stressed that the analysis devoted to the impact of changes in freshwater flux on deep mixing is based on detrended variables so that the results do not depend on the long-term climate change experienced over the 21st century, such as the long-term freshening of the high latitudes for instance.

After a brief description of the coupled climate model and its climatology in Section 2, the

processes responsible for the long-term freshening of the Arctic Ocean are examined in Section 3, while the link between inter-annual changes in freshwater fluxes and inter-annual convection depth anomalies over the 20th and 21st centuries is addressed in Section 4. Section 5 deals with the mechanisms influencing the long-term changes in the Fram Strait outflow. Conclusions are finally given in Section 6.

2. Model description and climatology

2.1 Model description and experimental set-up

We use the fourth version of the AOGCM developed at the "Institut Pierre Simon Laplace", Paris (IPSL-CM4, Marti et al., 2005). This model is made up of the atmospheric general circulation model LMDz (Hourdin et al., 2006), the oceanic general circulation model ORCA (Madec et al., 1998), the thermodynamic-dynamic sea ice model LIM (Fichefet et al., 1997) and the land surface scheme ORCHIDEE (Krinner et al., 2005). Time synchronisation and spatial interpolation of surface fluxes and variables between the atmospheric model and the three other components are ensured through the OASIS coupler (Valcke et al., 2004). There is no local flux correction in this model. The fresh water associated with ice sheet melting is drained toward the ocean and does not affect the ice sheet geometry (no dynamics). The atmospheric model has a horizontal resolution of 3.75° in longitude and 2.5° in latitude, with 19 levels along the vertical. The oceanic model has a coarse horizontal resolution of 2° in longitude and latitude, with vertical grid spacing increasing from 10 m in the top 150 m to 500 m at the bottom (31 levels).

The outputs from the experiment covering the 20th century, which includes only the anthropogenic forcing (observed CO_2 and sulphate aerosol concentrations) are first discussed. For the 21st century, we use outputs from the A1B climate change scenario as defined by the Special Report on Emission Scenarios, which corresponds to a continuous increase of CO_2 concentration until a level of about 720 ppm by 2100 (see Dufresne et al., 2005 for a more complete description of

those simulations).

2.2 Climatology of the Arctic Ocean

A detailed description of the model climatology can be found in Swingedouw et al. (2006). A summary is given here for the reader's convenience, with a particular focus on the Arctic Ocean. As most AOGCMs, IPSL-CM4 has several biases in its mean climate compared to observations. The AMOC index, defined as the maximum value of the annual mean meridional overturning streamfunction between 500 m and 5000 m depth in the Atlantic basin, is 11.8±0.7 Sv over the 20th century. This is somewhat weaker than the observational estimates of 15±2 Sv reported by Ganachaud and Wunsch (2000). Swingedouw et al. (2006) mostly attributed this error to an excessive precipitation less evaporation forcing between 45° and 50°N, which leads to too low sea surface salinities (SSS) in the northern North Atlantic. In the Labrador Sea, this results in the formation of a strong halocline that prevents winter deep oceanic convection. Deep convection sites in the model rather occurs in the GIN Seas in agreement with observations (Dickson et al., 1996) and south of Iceland, east of the southern tip of Greenland, with a maximum average ventilation depth of about 1200 m (Fig. 1). The good agreement between the simulated outflow rate of water denser than 27.8 kg m^{-3} over the Greenland-Iceland-Scotland ridge (5.4 Sv) and observations (5.6 Sv; Dickson et al., 1994) suggests that the AMOC bias is rather related to the absence of convection in the Labrador Sea (Swingedouw et al., 2006). This latter feature is accompanied by too large a sea ice extent in the Labrador Sea during winter (Fig. 2). In summer, however, the sea ice edge location agrees reasonably well with observations (Fig. 2). It should be noted that the too weak AMOC simulated by the model is also associated with a cold bias of about 5°C in the northern North Atlantic (45°-50°N).

The mean sea ice velocities computed by the model (not shown) are in reasonable agreement with those derived from the 85.5 GHz Special Sensor Microwave/Imager (SSM/I) data by Emery et

al. (1997). The sea ice drift features the Beaufort Gyre, the Transpolar Drift, the divergent motion on the Siberian shelf and the sea ice export through Fram Strait. The simulated large-scale ocean surface circulation (not shown) displays roughly the same features as the mean sea ice drift pattern in the Arctic Ocean, namely the Beaufort Gyre, the Transpolar Drift stream and the East Greenland Current. Both the Bering Strait inflow in the central Arctic (1 Sv) and the Canadian Archipelago throughflow (0.7 Sv) are close to observational data. In the GIN Seas, a cyclonic gyre is simulated, but the inflow of Atlantic waters into the Barents Sea appears too small (0.17 Sv) compared to observational estimates of Blindheim et al. (1989), which rather give about 3 Sv. This deficiency is mostly due to the too weak AMOC simulated by the model. The Fram Strait outflow (0.5 Sv) is therefore weaker than the one observed (3 Sv) in order to balance the mass budget of the central Arctic. Consequently, the modeled Arctic Ocean is somewhat isolated from the northern North Atlantic.

2.3 Simulated Arctic freshwater budget over 1951-2000

In the following, we describe the long-term mean of the volume-averaged freshwater balance of the Arctic Ocean over 1951-2000. This 50-year period has been chosen in order to avoid potential biases related to the large Arctic climate decadal variability in the model. The freshwater content in a given volume is defined as $\int (S_{ref}-S)dv \,/\, S_{ref}\, dv$ where S is the salinity and dv the volume increment. The reference salinity S_{ref} is fixed to 34.8 psu and corresponds to the volume-integrated salinity simulated by the model in the Arctic Ocean which we define as the area delineated by the Bering Strait and the 60^{th} parallel in the northern North Atlantic. The major contributions to the freshwater budget of the central Arctic Ocean, GIN Seas, and the region located south of Iceland are provided in Tables 1, 2 and 3 respectively while sea ice freshwater fluxes are given in Table 4. The geometry of those three regions is illustrated in Figure 3. It should be stressed that the link between freshwater fluxes and salinity is not straightforward. For example, a positive freshwater flux

directed toward a region of mean salinity smaller than the reference salinity could either increase or decrease the mean salinity depending of the magnitude of the freshwater flux, while when it is directed toward a region more saline than the reference salinity, then it always decreases the mean salinity of the considered region.

The largest source of freshwater in the central Arctic Ocean (Table 1) simulated by the model is the river runoff (R hereafter, 3456 km^3/yr) followed by the Bering Strait water inflow (2831 km^3/yr) and the atmospheric freshwater flux (precipitation less evaporation; 1136 km^3/yr; P-E hereafter). The magnitudes of these sources are close to estimates of Aagaard and Carmack (1989) (AC89 hereafter) for R and P-E and Woodgate and Aagaard (2005) for the Bering Strait water inflow. The model reproduces a sea ice export of 196 km^3/yr through Bering Strait whereas the observations rather show an inflow of 400 km^3/yr (Woodgate and Aagaard, 2005). Nevertheless, the total (i.e solid plus liquid) freshwater release (2635 km^3/yr) remains close to the estimation of Woodgate and Aagaard (2005) which is 2500 km^3/yr.

The largest sink of freshwater in the model central Arctic is the Fram Strait outflow (5034 km^3/yr) and is roughly equally partitioned between the solid and liquid contributions (Tables 1, 4). The annual mean ice export through Fram Strait is 93,400 m^3/s over 1951-2000, a value that compares quite well with data collected by Vinje et al. (1998) and Kwok et al. (2004). This yields a solid freshwater flux of 2581 km^3/yr, that matches the estimates of AC89. Although the simulated volume flux at Fram Strait (0.51±0.44 Sv) is roughly one-sixth of that observed, the liquid freshwater export there (2453 km^3/yr) exceeds the estimates of AC89 by about 1600 km^3/yr. This bias is mainly related to the too large liquid freshwater content (57,000 km^3), or the too low salinity, in the central Arctic Ocean in the model which overestimates the one estimated from the climatology of Levitus et al. (1994) by about 19,000 km^3.

The simulated inflow of salty waters from the North Atlantic toward the GIN Seas (-1543 km^3/yr) is underestimated by almost 50 percent compared to estimates of AC89 (-2880 km^3/yr).

Furthermore, both the simulated sea ice and liquid freshwater exports at Denmark Strait are overestimated by about 600 km^3/yr and 1200 km^3/yr respectively compared to observations of AC89, although the volume flux (5 Sv) be fairly realistic. Note that most of the biases underlined in this freshwater budget are likely related to the too weak AMOC simulated by the model and the subsequent too low salinity and temperature values in the northern North Atlantic.

In the GIN Seas (Table 2), the simulated river runoff (424 km^3/yr) and P-E (532 km^3/yr) are in reasonable agreement with observational estimates of AC89 (420 km^3/yr and 790 km^3/yr respectively). The sink of liquid freshwater in those seas is dominated by the freshwater export at Denmark Strait (-2116 km^3/yr) and the inflow of salty waters from the North Atlantic (-1543 km^3/yr), while the source of liquid freshwater is mainly due to the freshwater import through Fram Strait (2453 km^3/yr) and to the the sea ice to ocean freshwater flux (1826 km^3/yr).

South of Iceland, the sink of liquid freshwater (Table 3) is mainly caused by the inflow of salty waters originating from the North Atlantic (-7212 km^3/yr) and with a lower magnitude, by the export of liquid freshwater toward the Labrador Sea (-1603 km^3/yr). The source of freshwater south of Iceland is dominated by the inflow of freshwater through Denmark Strait (2116 km^3/yr) and the export of salty waters toward the GIN Seas (1543 km^3/yr). Note that P-E+R represents the third largest input of freshwater into the GIN Seas (956 km^3/yr) and into the region located south of Iceland (1406 km^3/yr) in the model during 1950-2000. Finally, the freshening of the deep Labrador Sea (2,300-3,300 m) identified over 1970-2000 by Dickson et al. (2002) appears also in the model but with a weaker magnitude (not shown).

3. Simulated changes in the Arctic freshwater budget over the 21st century

We briefly describe herein the changes experienced by the freshwater budget at high northern latitudes. In particular, we focus on the regions where deep-water formation takes place in

the model, namely the GIN Seas and the region located south of Iceland and on the central Arctic, which is the main source of freshwater for the surrounding seas (Fig. 3). It should be stressed that the Labrador Sea is excluded from our analysis since no deep convection occurs there in the model. In order to evaluate the changes in freshwater balance, we compare the period 2051-2100 of the SRES A1B experiment to the period 1951-2000. Individual contributions to the total liquid freshwater budget of the central Arctic, GIN Seas and region located south of Iceland averaged over a 50-year period to filter the decadal variability, are provided in Tables 1, 2 and 3 respectively, while sea ice freshwater fluxes are given in Table 4.

3.1 Central Arctic

The freshening of the central Arctic Ocean is dominated by the change in continental runoff, which has increased by about 2035 km^3/yr (0.065 Sv, 59%) between 1951-2000 and 2051-2100 (Table 1). This enhanced river discharge to the Arctic Ocean is an indication of the increase in the integrated high-latitude precipitation over continental areas resulting from an intensified hydrological cycle in response to global warming (Wu et al., 2002). The second most important change concerns the freshwater import through the northern boundary of the Barents Sea which has increased by 2020 km^3/yr. This is the contribution that experiences the largest relative change since near zero freshwater flux is simulated there over 1951-2000 (see Table 1). This large shift is due to the freshening of the GIN Seas and also to the strengthening of the northward mass transport through the Barents Sea. The increase in sea ice melting (1325 km^3/yr change) is the third largest source for the freshening of the central Arctic. Note that the sign of the ice-to-ocean freshwater flux is negative in the central Arctic, indicating that more ice is formed than melted there since it is exported. Finally, the change in the atmospheric freshwater flux (P-E) represents only a small contribution (358 km^3/yr) to the freshening of the central Arctic Ocean. Liquid freshwater export at Fram Strait over 2051-2100 is more than twice that simulated over 1951-2000 and appears to

dominate the sink of freshwater in the central Arctic (-5398 km^3/yr). The freshwater export through the Canadian Archipelago is enhanced by about 73% compared to 1951-2000, while the freshwater import through Bering Strait is decreased by about 25%. This latter feature is consistent with the freshening of the central Arctic. This freshening induces a decrease in the mean meridional pressure gradient between the Pacific and the central Arctic, which therefore weakens the Bering Strait throughflow (Coachman and Aagaard, 1966).

3.2 GIN Seas

Over 2051-2100, the linear trend of the annual mean freshwater content in the GIN Seas (315 km^3/yr) is much smaller than the one of the central Arctic Ocean (Table 2). The implications for deep-water formation are however significant as we will see later on. The largest change is related to the decrease of the northward inflow of salty waters originating from the North Atlantic (3718 km^3/yr change). Indeed, beyond year 2045 of the simulation, the inflow of Atlantic waters in the GIN Seas tends to decrease the average salinity of the GIN Seas rather than the opposite since the mid-latitudes of the North Atlantic become less saline than the Nordic seas. This source of freshening is nearly compensated by the increase of freshwater export at Denmark Strait which undergoes a shift of about 3500 km^3/yr (0.11 Sv). The increase in freshwater import at Fram Strait and the larger export to the Barents Sea represent the third and fourth largest changes, in absolute value, of the freshwater budget (2945 km^3/yr and -1866 km^3/yr respectively). Although sea ice melting occurs further upstream in the East Greenland Current over the second half of the 21st century compared to the 20th century, the freshwater flux into the ocean associated with sea ice melting/freezing decreases by 639 km^3/yr (35% change). This is related to a smaller inflow of ice from the Arctic through Fram Strait. Finally, local changes in P-E+R contribute only slightly to the long-term freshening of the GIN Seas (562 km^3/yr change). In summary, the changes in the freshwater fluxes between the GIN Seas and the surrounding oceans/seas dominate the changes in

the freshwater balance of the GIN Seas over the 21st century.

3.3 Region located south of Iceland

Although the linear trend of the annual mean freshwater content in this region is not significant over 2051-2100 (31 km^3/yr), large changes in freshwater fluxes are noticed (Table 3). The most noticeable modification is a decrease of the northward advection of salty waters originating from the North Atlantic which represents a source of freshening of 4707 km^3/yr. This is consistent with a reduced salinity in the North Atlantic (2 psu annual mean change between 1951-2000 and 2051-2100 at mid-latitudes) and and the weakening of the large-scale AMOC (5 Sv annual mean change by 2100 with respect to 1951-2000), which induce a reduced salt transport from low to high latitudes. This change is more than compensated by the increase of freshwater export to the Labrador Sea (5385 km^3/yr). The increase in P-E+R is weak and the ice-ocean freshwater flux has been reduced since less ice is transported through the Denmark Strait.

4. Links between changes in freshwater fluxes and inter-annual convection depth anomalies

As a consequence of the long-term freshening and warming of the Arctic Ocean, the model predicts that the convection almost disappears in the GIN Seas and south of Iceland by the end of the 21st century, with very shallow ventilation depth in March of about 100-200 m (not shown). However, this does not lead to a complete shut-down of the AMOC, as it remains at a value of about 6 Sv by 2100. In the following, we specifically focus on the processes promoting inter-annual deep convection anomalies in the GIN Seas and South of Iceland over the 20th and 21st centuries. We use detrended timeseries of annual mean freshwater fluxes and March mixed-layer depth which is used as a proxy for convection depth. The analysis is performed separately over 1901-1980 and

2021-2080. These peculiar periods have been chosen in order to avoid biases related to the linear detrend applied to the fields. The anomalies represent therefore the difference from the linear trend calculated over these two periods.

4.1 GIN Seas

4.1.1 20th century

Figure 4a shows that the correlation between March mixed layer depth anomalies in the GIN Seas and annual mean salinity anomalies averaged in the upper 100 m and over the East Greenland Current (EGC) region is slightly negative at zero lag. By contrast, a positive mixed layer depth anomaly tends to occur after relatively salty conditions in the eastern part of the GIN Seas. This indicates that the convection tends to be deep when the upper salinity in the EGC is low and when the upper levels of the eastern part of the GIN Seas are anomalously salty. Those features are in agreement with correlations depicted in Figure 5a. These latter show that the maximum of the mixed-layer depth in the GIN Seas occurs about two years after a minimum freshwater import from the North Atlantic. This is perfectly consistent with the idea that water mass formation in the GIN Seas results from the cooling of warm and salty waters originating from the North Atlantic. Note that the variations of upper salinity in the top 100 m in the eastern part of the GIN Seas are not related to the variations in the large-scale AMOC but rather to changes in the upper ocean circulation. Indeed, the maximum of the upper salinity there tends to occur one year after the minimum of the AMOC index with a correlation of -0.2. On the other hand, the convection depth reaches its maximum about 2 years after the maximum of the southward sea ice and liquid freshwater fluxes at Fram Strait, with a correlation of 0.4 (Fig. 5a). Indeed, almost all sea ice passing through Fram Strait melts close to Iceland over the 20th century. The subsequent freshwater anomalies are further advected to the North Atlantic and influence therefore weakly the deep

convection that takes place in the other parts of the GIN Seas. This is supported by the regression of winter mean (Dec-Feb) sea level pressure (SLP) upon the timeseries of annual mean Fram Strait outflow (Fig.6a) which is characterized by a maximum over Greenland. This pattern does not promote eastward advection of freshwater anomalies transported at Fram Strait toward the eastern part of the GIN Seas where deep convection takes place. As a consequence, the convection depth anomalies are not directly related to the influence of the freshwater transport at Fram Strait but rather to the atmospheric circulation anomalies as discussed below.

The anomalous winter mean atmospheric circulation associated to one standard deviation change in convection depth features stronger than usual north-easterly winds in the northern part of the GIN Seas and westerly winds in the southern part (Fig. 7a). This brings cold air from the Greenland ice sheet and the West Siberian shelf and induces large heat loss in the ice-free regions of the GIN Seas, therefore promoting deep convection there. Furthermore, this atmospheric pattern tends to increase the southward sea ice export through the Fram Strait and explains the positive correlation between sea ice export and mixed-layer depth at small negative lags (Fig. 5a).

In addition, when convection is strong, the GIN Seas are characterized by an anomalous cyclonic circulation in agreement with the wind-stress forcing and the large-scale geostrophic adjustment to density increase associated with convection (not shown). This circulation pattern tends to increase simultaneously the inflow of salty Atlantic waters and the southward liquid freshwater flux at Fram Strait, the sea ice export being rather controlled by local wind-stress forcing (Arfeuille et al., 2000, Vinje, 2001, Koenigk et al., 2005). This explains the almost phase opposition between correlations depicted in Fig. 5a.

The relationships described here strongly support the idea that inter-annual convection depth anomalies in the GIN Seas during the 20th century result from the anomalous atmospheric cooling of surface waters anomalously salty in agreement with observations. The coarse resolution of the model could have an influence on the representation of the processes described above as they do not

allow to accurately represent the lateral interactions between the East Greenland Current (EGC) and the remaining interior of the GIN Seas. Nevertheless, it should be mentioned that our results are consistent with those from other coarse-resolution coupled atmosphere-ocean models (e.g., Goosse et al., 2002). They are also coherent with the conclusions of Mauritzen and Hakkinen (1997), who showed, using a coupled ice-ocean model having a higher resolution that the present one, that the sea ice export at Fram Strait does not significantly influence convection in the GIN Seas.

4.1.2. 21st century

In contrast to the 20th century, the convection depth anomalies in the GIN Seas during the 21st century are strongly positively correlated (0.8) at lag -1 yr (convection lags) with the upper salinity anomalies averaged over the EGC (Fig 4b), and at zero lag with the upper salinity averaged in the eastern part of the GIN Seas. This indicates that, for this period, salinity anomalies transported in the EGC Seas could potentially induce changes in deep-water mass formation or amplify changes caused by other mechanisms. The correlations between convection depth anomalies and annual mean freshwater flux anomalies at Fram Strait and between Norway and Iceland over 2021-2080 are illustrated in Figure 5b. Similarly to the 20th century, a decrease of deep water formation in the GIN Seas tends to occur a few years after an increase in freshwater import from the North Atlantic. However, a noticeable difference from the 20th century, is that an increase of the deep water formation in the GIN Seas tends to occur a few years after a decrease of the solid and liquid freshwater export at Fram Strait during the 21st century. This behaviour might be related to the enhanced freshwater exchanges between the EGC and the interior of the GIN Seas. This idea is supported by the fact that the winter mean atmospheric circulation associated with a stronger than usual Fram Strait volume flux (Fig. 6b) displays westerly winds in the northern part of the EGC. This wind-stress forcing promotes the lateral exchanges of properties between the EGC and the interior of the GIN Seas and induces an increase in the eastward advection of positive sea ice

anomalies transported at Fram Strait. The subsequent melting of those sea ice anomalies further weaken the convection.

Additionally, the maximum freshwater export at Fram Strait occurs 4 years after the maximum of convection depth with a strong correlation of 0.8 (Fig 5b). This indicates that modifications of the freshwater export at Fram Strait during the 21st century might potentially be influenced by changes in convection in the GIN Seas. This contrasts with the 20th century during which a positive convection depth anomaly tends to occur after an increase in freshwater export at Fram Strait. Indeed, the winter mean atmospheric circulation associated with strong convection during the 21st century is characterized by southerly winds along the Norwegian coast and in the Barents-Kara Seas sector (Fig. 7b). This anomalous circulation first brings warm air from the North Atlantic to the Arctic Ocean. Second, it leads to larger than usual inflow of warm and salty waters in the eastern part of the GIN Seas and in the Barents-Kara Seas area. This could explain the higher correlation between convection depth anomalies and changes in northward inflow of salty waters over the 21st century compared to the 20th century (Fig. 5b). In addition to the anomalous northward advection of warm air and warm waters associated with strong convection, the temperature anomalies associated with ocean heat release induced by the convection itself are also transported northward in the Barents-Kara Seas sector. All these temperature anomalies then yield a decrease in sea ice cover in the Barents Sea that further warm the overlying atmosphere through the reduced insulating effect of sea ice in winter, the temperature-albedo feedback being very weak during that period of the year. Note that the changes in oceanic heat transport in the Barents Sea does not appear to be influenced by the large-scale AMOC, since the correlation between the maximum of the overturning streamfunction in the North Atlantic and the Barents Sea heat transport does not exceed 0.2 for all lags between -10 and +10 yr. This chain of processes is in agreement with the fact that an increase in surface air temperature (SAT) averaged over the Barents Sea occur after an increase in convection depth in the GIN Seas, with a maximum correlation of 0.8 at lag +4yr. It

should be mentioned that it has not been possible to establish a strong relationship between changes in convection and changes in the Barents Sea SAT during the 20th century. This can be inferred from the atmospheric circulation in Fig. 7a which does not promote an increase in the northward advection of warm air or warm waters in the Barents Sea when the convection is strong.

Let us examine the possible consequences of a positive SAT anomaly centered over the Barents Sea during the 21st century. The regression of the winter mean SLP anomalies upon the timeseries of the annual mean SAT anomalies averaged over the Barents Sea is characterized by a minimum around Spitzbergen with southward winds at Fram Strait and northeastward winds in the eastern part of the GIN Seas and in the Barents Sea (not shown). This anomalous atmospheric circulation induces more cyclonic conditions in the GIN Seas which induce a stronger than usual mass transport and freshwater export through Fram Strait that prevents deep convection, as suggested by the above correlation and regression analyses (Fig. 5b and 7b). An increase in freshwater export at Fram Strait tends therefore to occur after an increase in convection depth in the GIN Seas (Fig 5b). This feature is consistent with the correlation between the annual mean Barents Sea SAT and the annual mean liquid freshwater export at Fram Strait which reaches 0.8 at zero lag over 2021-2080. This negative SLP anomaly is also associated with southward advection of cold air from the central Arctic that tends to weaken the effect of freshwater on deep convection since salinity effects on deep convection overwhelm those associated with temperature. In addition, this anomalous atmospheric circulation tends to increase the oceanic heat transport in the Barents Sea which further amplifies the initial SAT anomaly in the Barents-Kara Seas through direct air-sea heat exchanges and intermediate sea ice processes (i.e. insulating effect in winter and temperature-albedo feedback in summer). Finally, advection of warm air from the North Atlantic into the Barents Sea sector by this anomalous atmospheric circulation amplifies also the initial SAT anomaly.

It should be mentioned that we cannot prove from our study if the northward ocean heat transport in the Barents Sea and the subsequent warming of the the atmosphere are able to influence

the SLP around Spitzbergen. However, the winter mean SLP pattern associated to one deviation standard change in Barents Sea SAT bears some resemblance with those obtained by Alexander et al. (2004) and Magnusdottir et al. (2004) who analyzed the response of the atmospheric circulation to realistic perturbations of SST and sea ice extent using stand-alone atmospheric general circulation models. Finally, the positive feedback found here between the Barents Sea SAT and the Barents Sea ocean heat transport was also recognized by Goosse and Holland (2005) in the second version of the Community Climate System Model (CCSM2) under present-day conditions with no changes in anthropogenic forcing.

To summarize, there is, during the 21st century a positive feedback between the Barents Sea ocean heat transport and the Barents Sea SAT and a negative one between the convection and the freshwater export at Fram Strait.

4.2 Region located south of Iceland

4.2.1 20th century

Fig 4c shows that the convection depth anomalies south of Iceland are negatively correlated with the upper salinity anomalies averaged in the Irminger Sea (the western part of the box 3) with a correlation of -0.2 at zero lag. This is in consistent with the correlations between changes in annual mean sea ice and liquid freshwater exports through the Denmark Strait and inter-annual convection depth anomalies (Fig. 5c). The convection depth reaches a maximum about one year after the maximum sea ice and liquid freshwater exports at Denmark Strait indicating that both solid and liquid freshwater fluxes are not the direct cause of the convection anomalies south of Iceland. This contrasts with the studies of Mauritzen and Hakkinen (1997), Hakkinen (1999) and Holland et al. (2001) who argued that convection in the North Atlantic is very sensitive to ice export through the Denmark Strait and its subsequent melting. However, the convection site in those modelling studies is located close to the southern tip of Greenland, a region which is directly affected by sea ice ex-

port through the Denmark Strait. By contrast, the deep-convection site located south of Iceland in our model is too far eastward of the EGC to be directly influenced by sea ice export through the Denmark Strait.

Close to the Denmark Strait, the annual mean atmospheric circulation associated with strong convection displays northerlies, as it can be deduced from SLP anomalies displayed in Fig. 8. This is consistent with larger than usual southward sea ice and freshwater transports there. In addition, this atmospheric pattern brings cold air from the central Arctic, which further enhances surface ocean heat loss to the atmosphere and thus promotes deep convection south of Iceland. Note that it was not possible to establish a coherent link between the behaviour of the freshwater fluxes at Denmark Strait when the convection is strong (Fig. 5c) and the regression of the winter mean SLP anomalies upon the timeseries of the annual mean convection depth anomalies (Fig. 7c).

In addition, the convection tends to be deep when the upper levels of the eastern part of the box 3 are anomalously salty, with a correlation of -0.5 at zero lag (Fig. 4c). This is coherent with the correlation between the convection depth anomalies and the changes in freshwater import from the North Atlantic which is strongly negative at zero lag (-0.8, Fig. 5c). Furthermore, the correlation between the convection anomalies and the annual variations in the northward mass flux in the eastern part of the box 3 peaks at +0.8 at zero lag. These features are in agreement with the regression of the winter mean SLP anomalies upon the timeseries of the annual mean convection depth anomalies (Fig. 7c). The associated wind-stress forcing induces a northward advection of salty waters originating from the North Atlantic in the convection site area. Finally, the changes in upper salinity in this region are mainly related to changes in the upper ocean circulation rather than variations in the large-scale AMOC. Indeed, the maximum upper salinity averaged in the upper 100 m tends to occur 2 years after a minimum of the AMOC index with a correlation of -0.3.

In summary, those results suggest that the inter-annual variability of convection depth south

of Iceland during the 20th century is related to the anomalous atmospheric cooling of waters anomalously salty originating from the North Atlantic.

4.2.2 21st century

Similarly to the GIN Seas, years characterized by strong convection south of Iceland during the 21st century tend to be associated with anomalously salty conditions in the upper levels of the Irminger Sea and of the eastern part of the box 3 (Fig. 4d). The correlations are however much higher than during the 20th century, suggesting than salinity changes could drive the convection depth anomalies during that period. Figure 5d illustrates the correlations between the maximum mixed layer depth and the freshwater exchanges at the Denmark Strait and with the North Atlantic. Similarly to the 20th century, the convection is weak two years after the maximum freshwater import from the North Atlantic with a correlation of -0.6 (Fig. 5d), and 2 years after the minimum northward volume flux. This is perfectly consistent with the winter mean atmospheric circulation associated with strong convection (Fig. 7d) which is characterized by north-easterly winds around the convection area, and the low salinity tongue located slightly northward of the souther limb of the sub-polar gyre and extending from off Newfoundland eastward at mid-latitudes of the North Atlantic. The large increase in freshwater export from the Arctic Ocean to the North Atlantic through the Canadian Archipelago (Table 1) and the Denmark Strait (Table 2) combined with the AMOC weakening and the enhanced hydrological cycle are likely to contribute to the formation of this low salinity tongue of about 30 psu during the 21st century. These features support thus the idea that the formation of positive convection depth anomalies south of Iceland during the 21st century results from the weaker than usual northward advection of fresh waters originating from the northwestern part of the North Atlantic.

It should be recalled at this stage that all the variables have been linearly detrended before performing the correlation analyses so that the results do not depend on the long-term climate

change experienced over the 21st century. The different relationships between inter-annual anomalies of convection and freshwater fluxes between the 20th and 21st centuries rather suggest that different mechanisms are involved. Finally, note that the spatial patterns of the correlation maps are similar to those of the regression maps in the GIN Seas and south of Iceland over the 20th century as well as over the 21st century (not shown). The correlations do not exceed 0.4 in most of the cases but are statistically significant at the 95% confidence level.

5. Processes influencing the long-term changes in the Fram Strait outflow

The export of sea ice and liquid freshwater through the Fram Strait strongly affects the deep water formation in the Labrador Sea and the circulation of the North Atlantic Ocean. It is therefore crucial to determine the mechanisms responsible for its long-term changes, and in particular in response to anthropogenic gas forcing. In this section, we specifically focus our analysis on the mechanisms influencing the long-term changes in liquid freshwater export at Fram Strait.

Figure 9 shows the timeseries of the liquid freshwater and volume fluxes at Fram Strait during the 20th and 21st centuries. An interesting feature seen in these timeseries is the rapid strengthening of the volume and freshwater fluxes between 1990 and 2010. Such an abrupt shift is not reproduced in a control simulation with pre-industrial conditions (Fig. 9). This means that the anthropogenic forcing is responsible for this significant change during that period. Furthermore, the volume and freshwater fluxes appear well correlated with a correlation coefficient up to 0.9 over 1901-1980 and 2021-2080 (all fields linearly detrended), suggesting that changes in the Fram Strait volume flux rather than changes in salinity have a significant influence on modifications of the liquid freshwater export at Fram Strait. We therefore investigate herein the mechanisms influencing the Fram Strait outflow rather than on those influencing the freshwater export.

5.1 Strengthening of the Fram Strait outflow

The large shift of the Fram Strait outflow simulated between 1990 and 2010 can be thought to be initiated by the reduction of sea ice cover in the Barents Sea which appears as a consequence of the long-term warming of the Arctic climate. The reduction of the annual mean sea ice cover in the Barents Sea over the late 20th century amplify the warming of the overlying atmosphere in this region mainly in winter through the reduced insulating effect of sea ice during that period. This yields a decrease of the mean SLP in winter around Spitzbergen that causes more cyclonic conditions in the GIN Seas. As a result, the Fram Strait outflow increases as well as the Barents Sea ocean heat transport which ultimately amplify the initial sea ice reduction. The increase in the ocean heat transport reaches 0.02 PW in annual mean between 1901-1980 and 2021-2080 (0.025 PW change in winter) and is similar to those obtained in several models poleward of 70°N in response to a doubling of the CO_2 (Holland and Bitz, 2003). In our model, the changes in Arctic surface air temperature in the Barents Sea between 1901-1980 and 2021-2080 are the largest over the Barents Sea with values up to 15°C in winter (9°C in annual mean, not shown). This regional amplification of the warming is consistent with the above positive feedback and the enhanced northward ocean heat transport in the Barents Sea. Finally, it should be noted that no similar shifts has been observed during the late 20th century although the variability of the exchanges between the North Atlantic and the GIN Seas through the Barents Sea has been large during the last decades.

5.2 Weakening of the Fram Strait outflow

Around year 2080, the model predicts a second transition threshold beyond which the Fram Strait outflow rapidly weakens (Fig. 9). There is indeed a competition between the positive feedback described above, that is responsible for the stability of state in which the Fram Strait outflow is large, and the geostrophic adjustment to the freshening in the GIN Seas which tends to

slow down the cyclonic circulation in the GIN Seas and thus the Fram Strait outflow. In agreement with the decrease of this latter, a strong halocline develops in the central Arctic during the course of the 21st century with an averaged annual mean SSS anomaly of almost 3 psu between 2080-2100 and 1901-1980. The slowing down of the cyclonic circulation in the GIN Seas is also associated with a reduced northward ocean heat transport in the Barents Sea. This contributes to an expansion of sea ice cover in this region as well as to a decrease of the SAT there. Averaged over the Barents Sea area, the surface air cooling reaches 5°C between 2080-2100 and 2021-2080, much higher than over the GIN Seas (1°C, not shown). Associated to this strong regional cooling is an increase of the winter mean SLP over the GIN Seas (6 hPa change) that amplifies the initial weakening of the cyclonic circulation in the GIN Seas caused by the long-term freshening.

There is therefore apparently a particular threshold beyond which the influence of the positive feedback between the Barents Sea SAT and the Barents Sea ocean heat transport is not sufficiently strong to sustain the Fram Strait outflow in a somewhat strong state against the freshening of the GIN Seas. Those results more or less suggest that there are two stable oscillatory states for Fram Strait outflow in the model because of those positive and negative feedbacks. Furthermore, the coarse resolution of our model does not allow to represent all currents, so that we reproduce only strong and weak modes, while in reality, the shape of the transition between these stable states could be more continuous.

Although those changes do not indicate causal relationships, they suggest the possibility that the long-term freshening in the GIN Seas could lead to strong regional cooling in a warming climate, through reorganization of horizontal ocean currents and heat transports in agreement with Russell and Rind (1999) and Schaeffer et al. (2002, 2004). Schaeffer et al. (2004) obtained a regional cooling south of Spitzbergen between 2060 and 2100 in response to the SRES A1B scenario. The area delineated by the decrease in SAT in their model coincides with the pattern of change in convection depth and expansion of sea ice. In our model however, the pattern of change

in SAT is centered over the Barents Sea, and coincides clearly with the area of expansion of sea ice, the convection changes being located southward in the interior of the GIN Seas. This indicates that the regional cooling in our model is rather ascribed to the insulating effect of sea ice rather than to a reduced ocean heat loss induced by a collapse of convection.

6. Conclusions

Outputs from IPSL-CM4 have been used to investigate the processes underlying the long-term changes of the freshwater balance of the high-latitude ocean in the Northern Hemisphere and the mechanisms influencing the formation of inter-annual convection depth anomalies over the 20th and 21st centuries. Additionally, the processes influencing the long-term evolution of the Fram Strait outflow have been examined. The analysis has been performed on the basis of simulations performed for the IPCC AR4, namely the experiment covering the 20th century, which includes only anthropogenic forcings, and the SRES A1B scenario over the 21st century.

In the central Arctic, the model predicts that changes in continental run-off dominate the long-term freshening over the 21st century, followed by increase in sea ice melting and increase in precipitation less evaporation. In the convection sites, localized in the GIN Seas and south of Iceland in our model, changes in oceanic freshwater fluxes rather than changes in P-E+R are seen to dominate the long-term change of the freshwater balance. We found that the Fram Strait outflow, which represents the main source of freshwater for the Nordic Seas, undergoes a large shift over the late 20th century. We suggest that this sudden transition is caused by a regional positive feedback in the atmosphere-sea ice-ocean system initiated by the retreat of sea ice cover in the Barents Sea as a result of the long-term warming of the Arctic climate. As the climate warms, the sea ice cover reduces in the Barents Sea. This amplifies the warming of the overlying atmosphere there which further increases the SLP over the GIN Seas. As a result the cyclonic ocean circulation in this region

strengthens as well as the Fram Strait outflow and the northward ocean heat transport in the Barents Sea that ultimately amplifies the initial sea ice reduction. Over the late 21st century, the model predicts a second transition threshold beyond which the Fram Strait outflow rapidly weakens. The long-term freshening in the GIN Seas, which affects directly the Fram Strait outflow and indirectly the magnitude of the overall above-mentioned positive feedback through its influence on the Barents Sea ocean heat transport, is pointed out as the main contender to explain this large shift.

Additionally, the mechanisms influencing the inter-annual changes in convection depth have been examined over the 20th and 21st centuries on the basis of correlation and regression analyses of detrended variables. This not allows to demonstrate causal effects or to assess the relative contributions of various processes in a particular phenomenon. Additional sensitivity experiments will thus be needed to illustrate the processes addressed herein. However, we were able to show that the mechanisms of inter-annual changes in deep convection in the GIN Seas and in the region located South to Iceland differ fundamentally between the 20th and 21st century. This difference is caused by the strong influence of the inter-annual changes in oceanic freshwater fluxes on the deep mixing during the 21st century. In particular, in the GIN Seas, during the 20th century, positive convection depth anomalies are related to atmospheric cooling of warm and salty waters originating from the North Atlantic in agreement with observations, whereas during the 21st century, modifications in the southward freshwater export through Fram Strait combined with changes in northward inflow of salty waters from the North Atlantic are seen to play a major role. Conversely, the convection depth anomalies in the GIN Seas during the 21st century influence the Fram Strait outflow through alterations of the sea level pressure around Spitzbergen. In the other convection site simulated by the model, south of Iceland, inter-annual convection depth anomalies during the 20th century are mostly related to atmospheric cooling as in the GIN Seas, whereas during the 21st century, modifications of the northward advection of fresh waters originating from the northwestern part of the North Atlantic have a significant influence.

It should be stressed that our analysis is based on a particular model using a coarse resolution which, as all climate models, shows several biases for present-day climate conditions. For instance, the "present-day" oceanic convection pattern simulated by our model is somewhat different from the one observed, with no deep-water production in the Labrador Sea. This bias could thus have an impact on the reliability of the Arctic climate change simulated by the model during the late 21st century. For example, Schaeffer et al. (2004) showed that the location of "present-day" convection sites in the ocean is crucial for the probability and strength of a regional cooling signal under global warming. In addition, our model does not include a comprehensive Greenland ice sheet model that has yet been shown to have a significant influence on the climate of the late 21st century (Fichefet et al., 2003).

Despite all the above-mentioned limitations and biases, several aspects of our results show consistency with previous published results obtained with different coupled models. This study suggests that the importance of oceanic freshwater fluxes in controlling the NADW formation at inter-annual time scales could significantly increase during the 21st century in response to increasing greenhouse gases, and that rapid climate transitions in the Arctic system could be trigger by moderate changes in the sea ice cover in the Barents Sea, an issue that must be kept in mind when analysing model results and observations in that region.

Acknowledgments.

H. Goosse is Research Associate with the Belgian National Fund for Scientific Research.
This work was conducted within the European project ENSEMBLES (ENSEMBLE-based Predictions of Climate Changes and their Impacts) and the Action Concertée Incitative Changement Climatique "Changement Climatique et Cryosphère" funded by the French Ministry of Research.

References

Alexander, M. A., U. S. Bhatt, J. E. Walsh, M. S. Timlin, J. S. Miller and J. D. Scott. (2004) The atmospheric response to realistic Arctic sea ice anomalies in an AGCM during winter. *J. Clim.,***17**, 890–905.

Aagaard, K. and E. C. Carmack (1989) The role of sea ice and other fresh water in the Arctic circulation, *J. Geophys. Res., 94, 14,485-14,498*

Arfeuille, G., L. A. Mysak and L.-B. Tremblay (2000) Simulation of the interannual variability of the wind-driven Arctic sea-ice cover 1958-1988, *Clim. Dyn., 16, 107-121.*

Arzel, O., T. Fichefet and H. Goosse (2006) Sea ice evolution over the 20th and 21st centuries as simulated by current AOGCMs, *Ocean Modelling, 12, 401-415*

Bengtsson, L., V. A. Semenov and O. A. Johanessen (2004) The early twientieth-century warming in the Arctic. A possible mechanism, *J. Clim., 17, 4045-4057*

Bitz, C. M. and G. H. Roe (2004) A mechanism for the high rate of sea ice thinning in the Arctic Ocean, *J. Clim., 17, 3223-3631*

Bryden, H. L., H. R. Longworth and S. A. Cunningham (2005) Slowing of the Atlantic meridional overturning circulation at 25N, *Nature, 438, 655-657*

Cavalieri, D. J., C. L. Parkinson and K. Y. Vinnikov (2003) 30-year satellite record reveals contrasting Arctic and Antarctic decadal sea ice variability, *Geophys. Res. Lett., 30, doi:10.1029/2003GL018931*

Curry, R., B. Dickson and I. Yashayaev (2003) A change in the freshwater balance of the Atlantic Ocean over the past four decades, *Nature, 426, 826-829*

Dickson, B., I. Yashayaev, J. Meincke, B. Turrell, S. Dye and J. Holfort (2002) Rapid freshening of the deep North Atlantic Ocean over the past four decades, *Nature, 416, 832-837*

Dickson, R. R. and J. Meincke and S. Malmberg and A. J. Lee (1988) The “Great Salinity Anomaly” in the northern North Atlantic, *Prog. in Oceanogr., 20, 103-151*

Dickson, K. W. and R. Brown (1994) The production of North Atlantic deep water – sources, rates and pathways, *J. Geophys. Res., 12:319-341.*

Dickson, R., J. Lazier, J. Meincke, P. Rhines and J. Swift (1996) Long-term coordinated changes in the convective activity of the North Atlantic, *Progress in Oceanography, 38, 241-295, 1996.*

Dufresne J-L, J. Quaas, O. Boucher, S. Denvil and L. Fairhead (2005) Contrasts in the effects on climate of anthropogenic sulfate aerosols between the 20th and the 21st century, *Geophys. Res. Lett.*, **32**, doi: 10.1029/2005GL023619

Emery, W. J., C. W. Fowler and J. A. Maslanik (1997) Satellite-derived maps of Arctic and

Antarctic sea ice motion: 1988 to 1994, *Geophys. Res. Lett., 24, 897-900*

Fichefet, T. and M. A. Morales Maqueda (1997) Sensitivity of a global sea ice model to the treatment of ice thermodynamics and dynamics, *J. Geophys. Res., 102, 12,609-12,646*

Fichefet, T., C. Poncin, H. Goosse, P. Huybrechts, I. Janssens and H. Le Treut (2003) Implications of changes in freshwater flux from the Greenland ice sheet for the climate of the 21st century, *Geophys. Res. Lett.,30, doi:10.1029/2003GL017826.*

Ganachaud, A. and C. Wunsch (2000) Improved estimates of global ocean circulation, heat transport and mixing from hydrographic data, *Nature, 407, 453-457*

Goosse, H., F. M. Selten, R. J. Haarsma and J. D. Opsteegh (2002) A mechanism of decadal variability of the sea-ice volume in the Northern Hemisphere, *Clim. Dyn., 19, 61-83*

Goosse, H. and M. Holland (2005) Mechanisms of decadal Arctic climate variability in the Community Climate System Model CCSM2, *J. Clim., 18, 3552-3570.*

Gregory, J. M., K. W. Dixon, R. J. Stouffer, A. J. Weaver, E. Driesschaert, M. Eby, T. Fichefet, H. Hasumi, A. Hu, J. H. Jungclaus, I. V. Kamenkovich, A. Levermann, M. Montoya, S. Murakami, S. Nawrath, A. Oka, A. P. Sokolov and R. B. Thorpe (2005) A model of intercomparison of changes in the Atlantic thermohaline circulation in response to increasing atmospheric CO_2 concentration, *Geophys. Res. Lett., 32, doi:10.1029/2005GL023209*

Hansen, B., W. R. Turrell and S. Osterhus (2001) Decreasing overflow from the Nordic seas into the Atlantic Ocean through the Faroe Bank channel since 1950, *Nature, 411, 927-930*

Hakkinen, S. (1999) A Simulation of thermohaline effects of a great salinity anomaly, *J. Clim, 12, 1781-1795*

Holland, M. M. and C. M. Bitz (2003) Polar amplification of climate change in coupled models, *Clim. Dyn., 21, 221-232.*

Holland, M. M., C. M. Bitz, M. Eby, A. Weaver (2001) The role of ice-ocean interactions in the variability of the North-Atlantic thermohaline circulation

Houghton, J. T. and Coauthors (2001) IPCC 2001, Climate Change (2001) The scientific basis, Contribution of Working Group 1 to the third assessment report of Intergovernmental Panel on Climate Change. 881 pp., Cambridge University Press, Cambridge, United Kingdom and New York, USA.

Hourdin, F., I. Musat, S. Bony, P. Braconnot, F. Codron, J.-L. Dufresne, L. Fairhead, M-A. Filiberti, P. Friedlingstein, J.-Y. Grandpeix, G. Krinner, P. LeVan, Z.X. Li and F. Lott (2006) The LMDZ4 general circulation model: climate performance and sensitivity to parameterized physics with emphasis on tropical convection, *Clim. Dyn.*, **19**, 3445-3482

Johannessen, O. M., L. Bengtsson, M. W. Miles, S. I. Kuzmina, V. A. Semenov, G. V. Alekseev, A. P. Nagurnyi, V. F. Zakharov, L. P. Bobylev, L. H. Pettersson, K. Hasselmann, H. P. Cattle (2004) Arctic climate change - Observed and modeled temperature and sea ice variability, *Tellus, 56A,*

328-341

Jungclaus, J. H, H. Haak, U. Mikolajewicz and M. Latif (2005) Arctic-North Atlantic interactions and multidecadal variability of the meridional overturning circulation, *J. Clim, 18, 4016-4034*

Krinner, G., N. Niovy, N. Noblet-Ducoudré, J. Ogée, J. Polcher, P. Friedlingstein, P. Ciais, S. Sitch, and I. C. Prentice (2005) A dynamic global vegetation model for studies of the coupled atmosphere-biosphere system, *Glob. Biogeochem. Cycles, 19, GB1015, doi: 10.1029/2003GB002199*

Koenigk, T., U. Mikolajewicz, H. Haak, J. Jungclaus (2005) Variability of Fram Strait sea ice export: causes, impacts and feedbacks in a coupled climate model

Kwok, R., G. F. Cunningham and S. S. Pang (2004) Fram Strait sea ice outflow, *J. Geophys. Res., 109, doi:10.1029/2003JC001785*

Levitus, S., R. Burgett and T.P. Boyer (1994) World Ocean Atlas 1994. Volume 3: Salinity. *NOAA Atlas NESDIS 3. U.S. Deptartment of Commerce. Washington, D.C.*

Madec, G., P. Delecluse, M. Imbard, M. Lévy (1998) OPA 8.1, Ocean General Circulation Model reference manual, *Notes du pôle de modélisation, Institut Pierre-Simon Laplace (IPSL), France,* **11**, 91pp

Magnusdottir, G., C. Deser and R. Saravanan (2004) The effects of North Atlantic SST and Sea ice anomalies on the winter circulation in CCM3. Part I: Main features and storm track characteristics of the response. *J. Clim.*, **17**, 857–876.

Manabe, S. and R. J. Stouffer (1995) Simulation of abrupt climate change induced by fresh-water input into the North Atlantic Ocean, *Nature, 378, 165-167.*

Marti, O., P. Braconnot, J. Bellier, R. Benshila, S. Bony, P. Brockmann, P. Cadule, A. Caubel, S. Denvil, J.-L. Dufresne, L. Fairhead, M. A, Filiberti, M.-A. Foujols, T. Fichefet, P. Friedlingstein, H. Goosse, J.-Y. Grandpeix, F. Hourdin, G. Krinner, C. Lévy, G. Madec, I. Musat, N. de Noblet, J. Polcher and C. Talandier (2005) The new IPSL climate system model: IPSL-CM4, *Note du pôle de modélisation, 26, ISSN 1288-1619, 2005. http://igcmg.ipsl.jussieu.fr/Doc/IPSLCM4/*

Mauritzen, C. and S. Hakkinen (1997) Influence of sea ice on the thermohaline circulation in the Arctic-North Atlantic Ocean, *Geophys. Res. Lett., 24, 3257-3260.*

Moritz, R. E., C. M. Bitz and E. J. Steig (2002) Dynamics of recent climate change in the Arctic, *Science, 297, 1497-1502*

Overland, J. E., M. C. Spillane and N. N. Soreide (2004) Integrated analysis of physical and biological pan-Arctic change, *Clim. Chg., 63, 291-322*

Peterson, B. J., R. M. Holmes, J. W. McClelland, C. J. Vorosmarty, R. B. Lammers, A. I. Shiklomanov, I. A. Shiklomanov and S. Rahmstorf (2002) Increasing river discharge to the Arctic Ocean, *Science, 298, 2171-2173*

Polyakov, I. V. and M. A. Johnson (2000) Arctic decadal and interdecadal variability, *Geophys.*

Res. Lett., 27, 4097-4100

Polyakov, I. V., G. V. Alekseev, R. V. Bekryaev, U. Bhatt, R. L. Colony, M. A. Johnson, V. P. Karklin, A. P. Makshtas, D. Walsh and A. V. Yulin (2002) Observationally based assessment of polar amplification of global warming, *Geophys. Res. Lett., 29, doi:10.1029/2001GL011111.*

Rayner, N. A., D. E. Parker, E. B. Horton, C. K. Folland, L. V. Alexander, D. P. Rowell, E. C. Kent and A. Kaplan (2003) Global analyses of sea surface temperature, sea ice, and night marine air temperature since the late nineteenth century, *J. Geophys. Res, 108, doi:10.1029/2000JC000542*

Rothrock, D. A., Y. Yu and G. A. Maykut (1999) Thinning of the Arctic sea ice cover, *Geophys. Res. Lett., 26, 3469-3472*

Russel, G. L. and D. Rind (1999) Response to CO_2 transient increase in the GISS coupled model: regional coolings in a warming climate*, J. Clim.*, **12**, 531-539

Schaeffer, M., F. M. Selten, J. D. Opsteegh (2002) Intrinsic limits to predictability of abrupt regional climate change in IPCC SRES scenarios, *Geophys. Res. Lett., 29, doi:10.1029/2002GL015254.*

Schaeffer, M., F. M. Selten, J. D. Opsteegh and H. Goosse (2004) The influence of ocean convection patterns on high-latitude climate projections, *J. Clim., 17, 4316-5329*

Serreze, M. C. and Coauthors (2000) Observational evidence of recent change in the northern high-latitude environment, *Clim. Chg., 46, 157-207*

Swingedouw, D., P. Braconnot, P. Delecluse, E. Guilyardi and O. Marti (2006) Sensitivity of the Atlantic thermohaline circulation to global freshwater forcing, *submitted to Clim. Dyn.*

Valcke, S., D. Declat, R. Redler, H. Ritzdorf, T. Schoenemeyer, R. Vogelsang (2004) Proceedings of the 6th International Meeting: High performance computing for computational science, *Universidad Politecnica de Valencia, Valencia, Spain. The PRISM Coupling and I/O System. VECPAR'04*

Vellinga, M. and R. A. Wood (2002) Global climatic impacts of a collapse of the Atlantic thermohaline circulation, *Clim. Change, 54, 251-267.*

Vinje, T., N. Nordlund and A. Kvambekk (1998) Monitoring ice thickness in Fram Strait, *J. Geophys. Res., 103, 10,437-10,449*

Vinje, T. (2001) Fram Strait ice fluxes and atmospheric circulation 1950-2000, *J. Clim, 14, 3508-3517.*

Woodgate, R. E. and K. (2005) Revising the Bering Strait freshwater flux into the Arctic Ocean, *Geophys. Res. Lett., 32, doi:10.1029/2004GL021747*

Wu, P., R. Wood and P. Stott (2004) Does the recent freshening trend in the North Atlantic indicate a weakening of the thermohaline circulation ?, *Geophys. Res. Lett., 31, doi:10.1029/*2003GL018584

Figures captions

Figure 1. Simulated mixed layer depth in March averaged over 1951-2000 (m). Contour interval is 100 m.

Figure 2. Sea ice concentrations in March (left) and September (right) simulated by IPSL-CM4 averaged over 1951-2000. Contour interval is 0.1. The observed sea ice edge, defined as the 15% concentration for March and September is derived from the HadISST dataset (Rayner et al., 2003) and shown as a thick solid line.

Figure 3. Geometry of the three boxes chosen for the analysis. These include the central Arctic (box 1), the Greenland-Iceland-Norwegian Seas (box 2) and the region located to the south of Iceland (box 3). These two latter enclose the region where the convection sites are located over the 20th century (see Fig. 1).

Figure 4. Correlations between the March mixed-layer depth anomalies and the annual mean salinity anomalies averaged in the upper 100 m in the GIN Seas as a function of lag over 1901-1980 (a) and 2021-2080 (b). Solid contours indicate the correlation between mixed layer depth and upper salinity averaged in the eastern part of GIN Seas which correspond to the areas where deep convection takes place. Dashed contours indicate the correlation between mixed layer depth and upper salinity averaged in the East Greenland Current (a-b) and in the Irminger Sea (the western part of the box 3, c-d). A linear detrend and a 5-yr running mean have been performed. Mixed layer depth anomaly lags (leads) the salinity anomaly for negative (positive) lags.

Figure 5. (a-b) Correlation between March convection depth anomalies in the GIN Seas and annual mean liquid freshwater flux through Fram Strait (solid), annual mean sea ice transport through Fram Strait (dashed) and liquid freshwater import from North Atlantic (solid dotted) as a function of lag over 1901-1980 (a) and 2021-2080 (b). (c-d) Correlation between March convection depth anomalies South of Iceland and annual mean liquid freshwater flux through Denmark Strait (solid), annual mean sea ice transport through Denmark Strait (dashed) and liquid freshwater import from the North Atlantic (solid dotted) as a function of lag over 1901-1980 (c) and 2021-2080 (d). A linear detrend and a 5-yr running mean have been performed before the analysis. Mixed layer depth anomaly lags (leads) the anomalous freshwater fluxes for negative (positive) lags.

Figure 6. Winter mean (DJF) SLP (hPa) regressed upon the timeseries of the annual mean Fram Strait transport over 1901-1980 (a) and 2021-2080 (b) at zero lag. Shown is the change of SLP related to one standard deviation change in annual mean Fram Strait transport. Contour interval is 0.2 hPa. A linear detrend has been perfomed for SLP and Fram Strait transport. Negative values are dashed.

Figure 7. Winter mean (DJF) SLP (hPa) regressed upon the timeseries of the March mixed-layer depth in the GIN Seas and in the region South of Iceland over 1901-1980 and 2021-2080. Shown is the change of SLP related to one standard deviation change in March mixed-layer depth. Contour interval is 0.2 hPa. A linear detrend has been performed for SLP and mixed-layer depth. Negative values are dashed.

Figure 8. Annual mean SLP (hPa) regressed upon the timeseries of the March mixed-layer depth in the region South of Iceland over 1901-1980. Shown is the change of SLP related to one standard

deviation change in March mixed-layer depth. Contour interval is 0.2 hPa. A linear detrend has been performed for SLP and mixed-layer depth. Negative values are dashed.

Figure 9. The timeseries of (top) Fram Strait outflow and (bottom) liquid freshwater export at Fram Strait. A 5-year running mean has been performed. The thin line denotes the timeseries associated to the pre-industrial experiment, while the thick solid line denotes the timeseries associated to the experiment covering the 20th century with anthropogenic forcings and the SRES A1B scenario over the 21st century.

List of tables

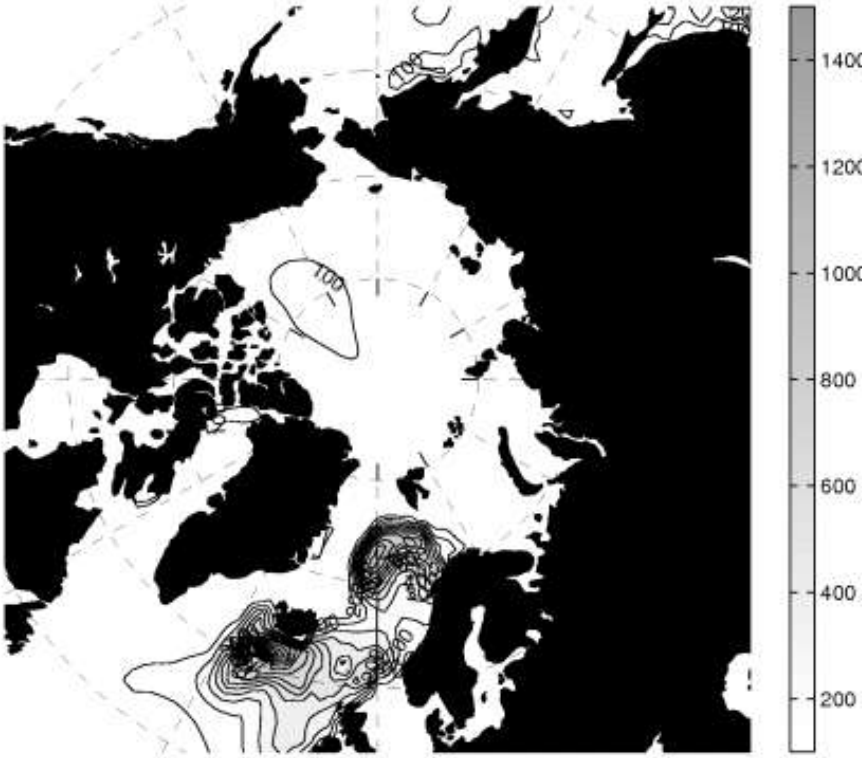

Figure 1. Simulated mixed layer depth in March averaged over 1951-2000 (m). Contour interval is 100 m.

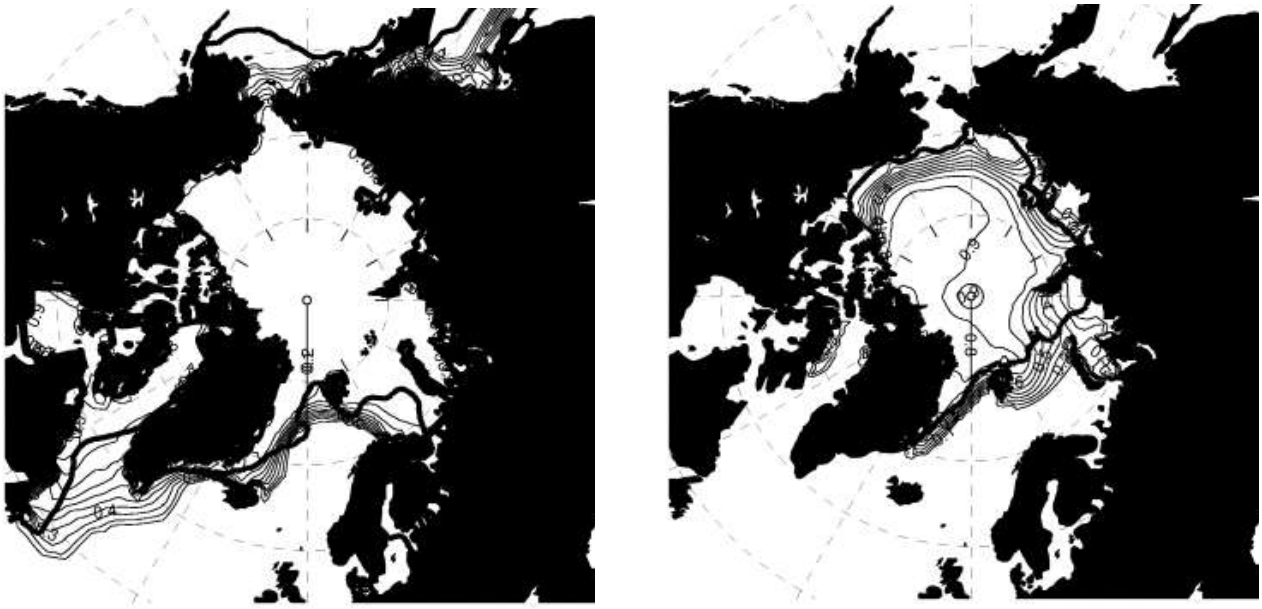

Figure 2. Sea ice concentrations in March (left) and September (right) simulated by IPSL-CM4 averaged over 1951-2000. Contour interval is 0.1. The observed sea ice edge, defined as the 15% concentration for March and September is derived from the HadISST dataset (Rayner et al., 2003) and shown as a thick solid line.

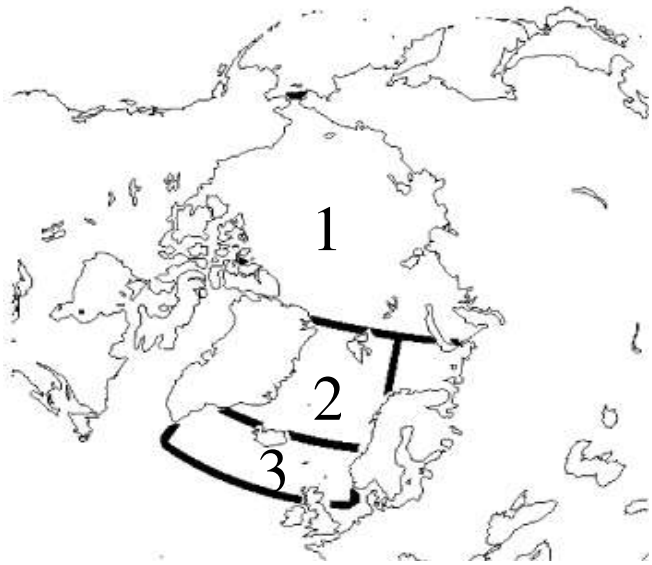

Figure 3. Geometry of the three boxes chosen for the analysis. These include the central Arctic (box 1), the Greenland-Iceland-Norwegian Seas (box 2) and the region located to the south of Iceland (box 3). These two latter enclose the region where the convection sites are located over the 20th century (see Fig. 1).

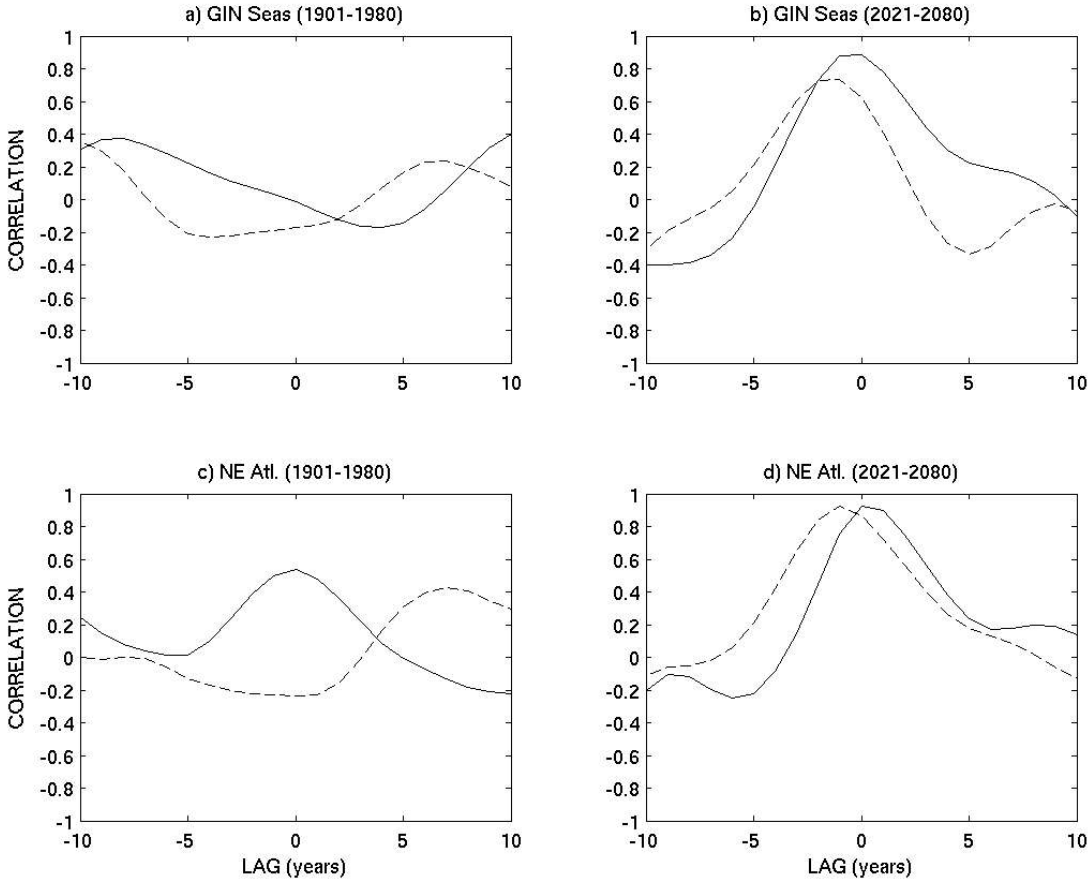

Figure 4. Correlations between the March mixed-layer depth anomalies and the annual mean salinity anomalies averaged in the upper 100 m in the GIN Seas as a function of lag over 1901-1980 (a) and 2021-2080 (b). Solid contours indicate the correlation between mixed layer depth and upper salinity averaged in the eastern part of GIN Seas which correspond to the areas where deep convection takes place. Dashed contours indicate the correlation between mixed layer depth and upper salinity averaged in the East Greenland Current (a-b) and in the Irminger Sea (the western part of the box 3, c-d). A linear detrend and a 5-yr running mean have been performed. Mixed layer depth anomaly lags (leads) the salinity anomaly for negative (positive) lags.

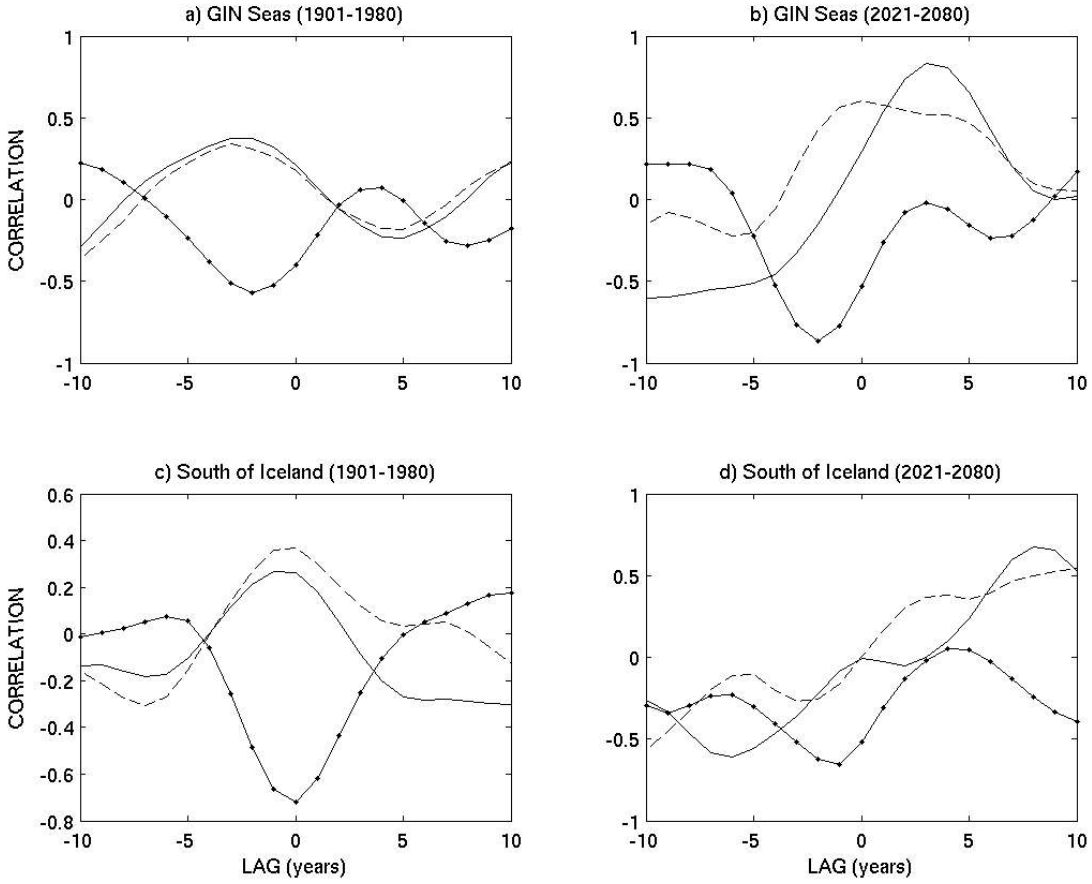

Figure 5. (a-b) Correlation between March convection depth anomalies in the GIN Seas and annual mean liquid freshwater flux through Fram Strait (solid), annual mean sea ice transport through Fram Strait (dashed) and liquid freshwater import from North Atlantic (solid dotted) as a function of lag over 1901-1980 (a) and 2021-2080 (b). (c-d) Correlation between March convection depth anomalies South of Iceland and annual mean liquid freshwater flux through Denmark Strait (solid), annual mean sea ice transport through Denmark Strait (dashed) and liquid freshwater import from the North Atlantic (solid dotted) as a function of lag over 1901-1980 (c) and 2021-2080 (d). A linear detrend and a 5-yr running mean have been performed before the analysis. Mixed layer depth anomaly lags (leads) the anomalous freshwater fluxes for negative (positive) lags.

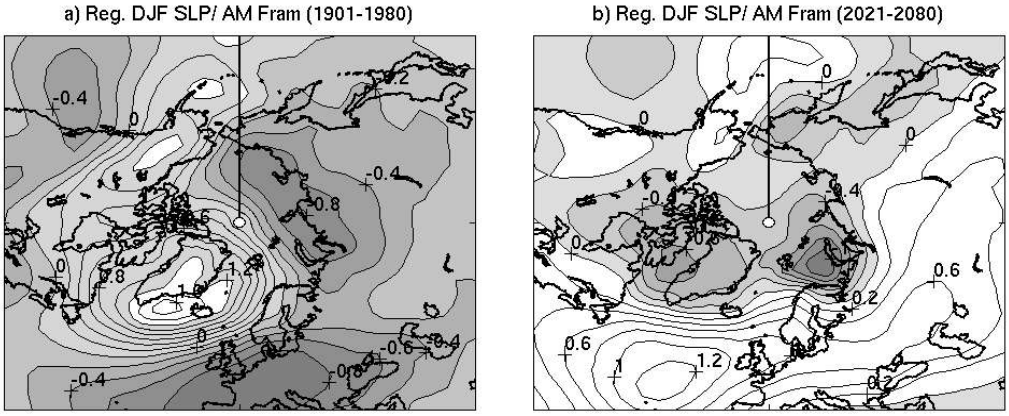

Figure 6. Winter mean (DJF) SLP (hPa) regressed upon the timeseries of the annual mean Fram Strait transport over 1901-1980 (a) and 2021-2080 (b) at zero lag. Shown is the change of SLP related to one standard deviation change in annual mean Fram Strait transport. Contour interval is 0.2 hPa. A linear detrend has been perfomed for SLP and Fram Strait transport. Negative values are dashed.

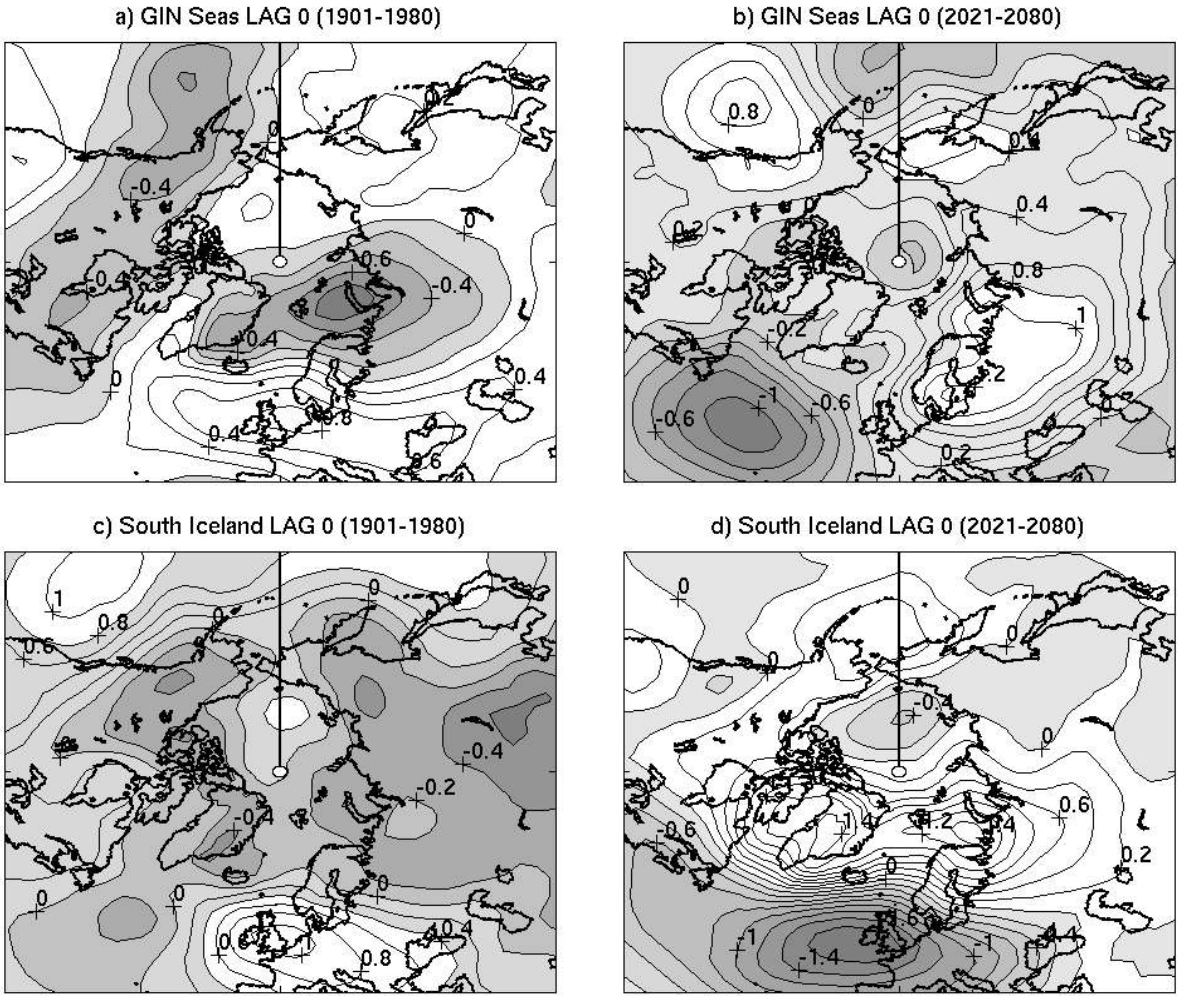

Figure 7. Winter mean (DJF) SLP (hPa) regressed upon the timeseries of the March mixed-layer depth in the GIN Seas and in the region South of Iceland over 1901-1980 and 2021-2080. Shown is the change of SLP related to one standard deviation change in March mixed-layer depth. Contour interval is 0.2 hPa. A linear detrend has been performed for SLP and mixed-layer depth. Negative values are dashed.

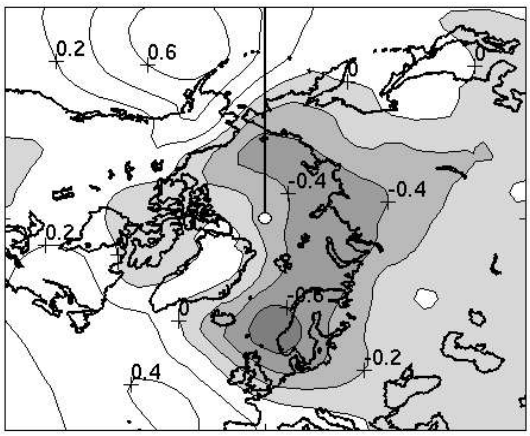

Figure 8. Annual mean SLP (hPa) regressed upon the timeseries of the March mixed-layer depth in the region South of Iceland over 1901-1980. Shown is the change of SLP related to one standard deviation change in March mixed-layer depth. Contour interval is 0.2 hPa. A linear detrend has been performed for SLP and mixed-layer depth. Negative values are dashed.

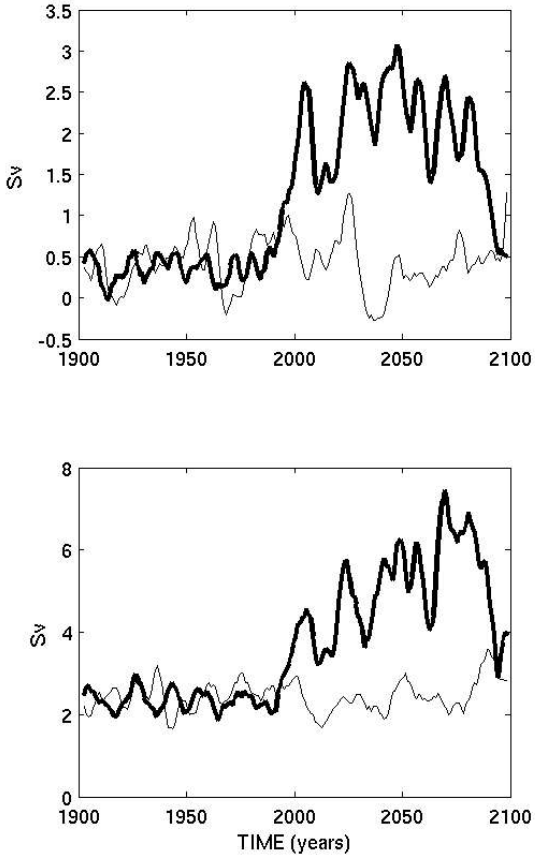

Figure 9. The timeseries of (top) Fram Strait outflow and (bottom) liquid freshwater export at Fram Strait. A 5-year running mean has been performed. The thin line denotes the timeseries associated to the pre-industrial experiment, while the thick solid line denotes the timeseries associated to the experiment covering the 20th century with anthropogenic forcings and the SRES A1B scenario over the 21st century.

	Observations	1951-2000	2051-2100	change
Linear trend of annual mean freshwater content		299	1754	1455
P-E	900 (AC89)	1136	1494	358
R	3300 (AC89)	3456	5491	2035
Ice to Ocean freshwater flux		-2737	-1412	1325
Freshwater export at Fram Strait	-820 (AC89)	-2453	-5398	-2945
Freshwater export through Canadian Archipelago	-920 (AC89)	-1329	-2299	-970
Freshwater import at Bering Strait	2070 (WA05)	2831	2126	-705
Freshwater import from Barents Sea	-540 (AC89)	1	2021	2020

Table 1. Annual mean freshwater budget in the central Arctic Ocean averaged over the period 2051-2100 of the SRES A1B experiment (km^3/yr). Corresponding change between 1951-2000 and 2051-2100 is indicated in the right column. Freshwater fluxes are relative to the reference salinity 34.8 psu. Positive values are for sources and negative ones for sinks. Acronyms AC89 and WA05 state for Aagaard and Carmack (1989) and Woodgate and Aagaard (2005).

	Observations	1951-2000	2051-2100	Change
Linear trend of annual mean freshwater content		34	315	281
P-E	790 (AC89)	532	573	41
R	420 (AC89)	424	945	521
Ice to ocean freshwater flux		1826	1187	-639
Freshwater import at Fram Strait	820 (AC89)	2453	5398	2945
Freshwater export to Barents Sea	544 (AC89)	463	-1403	-1866
Freshwater export at Denmark Strait	-900 (AC89)	-2116	-5603	-3487
Freshwater import from North Atlantic	-2880 (AC89)	-1543	2175	3718

Table 2. Annual mean freshwater budget in the GIN Seas for the ocean averaged over the period 1951-2000 in the model and observations, and over 2051-2100 of the SRES A1B experiment (km^3/yr). Corresponding change between 1951-2000 and 2051-2100 is indicated in the right column. Freshwater fluxes are relative to the reference salinity 34.8 psu. Positive values are for sources and negative ones for sinks. Acronym AC89 state for Aagaard and Carmack (1989).

	Observations	1951-2000	2051-2100	Change
Linear trend of annual mean freshwater content		-48	31	79
P-E		868	1015	477
R		538	1135	267
Ice to ocean freshwater flux		909	146	-763
Freshwater import at Denmark Strait	900 (AC89)	2116	5603	3487
Freshwater export to GIN Seas	2880 (AC89)	1543	-2175	-3718
Saline water import from North Atlantic		-7212	-2505	4707
Freshwater export to Labrador Sea		-1603	-6989	-5386

Table 3. Annual mean freshwater budget in the region south of Iceland for the ocean (see Figure 3) averaged over the period 1951-2000 in the model and available observations, and over 2051-2100 of the SRES A1B experiment (km^3/yr). Corresponding change between 1951-2000 and 2051-2100 is indicated in the right column. Freshwater fluxes are relative to the reference salinity 34.8 psu. Saline waters are referred to salinities greater than 34.8 psu (i.e. the reference salinity). Positive values are for sources and negative ones for sinks. Acronym AC89 state for Aagaard and Carmack (1989).

	Observations	1951-2000	2051-2100	Change
Fram Strait	-2790 (AC89)	-2581	-1691	890
Denmark Strait	-560 (AC89)	-1129	-112	1017
Bering Strait	400 (WA05)	-196	-52	144
Canadian Archipelago	-155 (AC89)	-396	-173	223

Table 4. Annual mean sea ice (solid) freshwater flux in the Arctic Ocean and in observations, averaged over 1951-2000 and 2051-2100 in the model (km^3/yr). Corresponding change between 1951-2000 and 2051-2100 is indicated in the right column. Negative sign indicates a southward sea ice export. AC89 states for Aagaard and Carmarck (1989) and WA05 states for Woodgate and Aagaard (2005). The freshwater flux are computed assuming a mean salinity of ice of 4 psu and a reference salinity of 34.8 psu.